JID Open

A Three-Dimensional Atlas of Human Dermal Leukocytes, Lymphatics, and Blood Vessels

Xiao-Nong Wang[1], Naomi McGovern[1], Merry Gunawan[1], Connor Richardson[1], Martin Windebank[1], Tee-Wei Siah[2], Hwee-Ying Lim[3], Katja Fink[4], Jackson L. Yao Li[4], Lai G. Ng[4], Florent Ginhoux[4], Veronique Angeli[3], Matthew Collin[1] and Muzlifah Haniffa[1]

Dendritic cells (DCs), macrophages (Mϕ), and T cells are major components of the skin immune system, but their interstitial spatial organization is poorly characterized. Using four-channel whole-mount immunofluorescence staining of the human dermis, we demonstrated the three-dimensional distribution of $CD31^+$ blood capillaries, $LYVE\text{-}1^+$ lymphatics, discrete populations of $CD11c^+$ myeloid DCs, $FXIIIa^+$ Mϕ, and lymphocytes. We showed phenotypic and morphological differences *in situ* between DCs and Mϕ. DCs formed the first dermal cellular layer (0–20 μm beneath the dermoepidermal junction), Mϕ were located deeper (40–60 μm), and $CD3^+$ lymphocytes were observed throughout (0–60 μm). Below this level, DCs, T cells, and the majority of Mϕ formed stable perivascular sheaths. Whole-mount imaging revealed the true extent of dermal leukocytes previously underestimated from cross-section views. The total area of apical dermis (0–30 μm) contained approximately 10-fold more myeloid DCs than the entire blood volume of an average individual. Surprisingly, <1% of dermal DCs occupied lymphatics in freshly isolated skin. Dermal DCs rapidly accumulated within lymphatics, but Mϕ remained fixed in skin explants cultured *ex vivo*. The leukocyte architecture observed in normal skin was distorted in inflammation and disease. These studies illustrate the micro-anatomy of dermal leukocytes and provide further insights into their functional organization.

Journal of Investigative Dermatology (2014) **134,** 965–974; doi:10.1038/jid.2013.481; published online 19 December 2013

INTRODUCTION

The human dermis is rich in leukocytes such as dendritic cells (DCs), macrophages (Mϕ), and T cells. Skin DCs migrate to lymph nodes to activate naive T cells, but there is evidence to suggest that skin DCs and Mϕ may also interact with memory T cells *in situ* (Tomura *et al.*, 2010; Jiang *et al.*, 2012). Skin DCs comprise distinct subsets. In addition to $CD1a^{++}$ $Langerin^+$ epidermal Langerhans cells (LCs), $CD1c^+$ DCs co-expressing CD1a, $CD14^+$ DCs, and $CD141^{hi}XCR1^+$ DCs have been identified (Czernielewski *et al.*, 1983; Lenz *et al.*, 1993; Nestle *et al.*, 1993; Haniffa *et al.*, 2012 and reviewed in Collin *et al.*, 2013) and distinguished from $FXIIIa^+CD163^+$ interstitial Mϕ (Haniffa *et al.*, 2009; Zaba *et al.*, 2009). Dermal DC subsets have distinct cytokine profiles and are functionally specialized (Morelli *et al.*, 2005; Klechevsky *et al.*, 2008; Haniffa *et al.*, 2012). Dermal T cells are predominantly $CD4^+$, have the effector memory cell phenotype ($CD45RA^-CD45RO^+CCR7^-$), express the skin addressins CLA, CCR6, and CCR4, and possess a diverse TCR repertoire (Clark *et al.*, 2006a, b). Th1, Th2, Th17, and Th22 $CD4^+$ T cells have been described (Eyerich *et al.*, 2009 and reviewed in Sallusto *et al.*, 2012). $CD4^+CD25^{hi}$ regulatory T cells are observed in the dermis and are shown to be modulated by epidermal LCs (Clark, 2010; Seneschal *et al.*, 2012). Animal studies have shown antigen-presenting cells (APCs) and T-cell migration into skin via blood vessels and to the draining lymph node via lymphatic channels (reviewed in Forster *et al.*, 2012).

Studies on human skin leukocytes, blood, and lymphatic conduits have relied on two main techniques: (i) flow cytometry of cells migrated from skin explant cultured *ex vivo* or digested skin and (ii) *in situ* microscopic analysis of cross-sectioned skin (Ochoa *et al.*, 2008; Zaba *et al.*, 2009). These studies lacked the resolution to illustrate dermal vascular networks, microanatomy of skin leukocytes, and the role of lymphatics as conduits for DC migration to the draining lymph node (Hudack and McMaster, 1933; Zaba *et al.*, 2007; Ochoa *et al.*, 2008).

Here we performed whole-mount dermal sheet microscopy to analyze DCs, Mϕ, and T cells in normal and diseased skin. We also analyzed dermal blood and lymphatic vessels and interrogated dermal APC lymphatic migration capacity in normal skin. This study provides further insights into the

[1]*Institute of Cellular Medicine, Newcastle University, Newcastle upon Tyne, UK;* [2]*Department of Dermatology, Royal Victoria Infirmary, Newcastle upon Tyne, UK;* [3]*National University of Singapore, Singapore, Singapore and* [4]*Singapore Immunology Network, A*Star, Singapore, Singapore*

Correspondence: Muzlifah Haniffa or Xiao-Nong Wang, Institute of Cellular Medicine, Newcastle University, Newcastle upon Tyne NE2 4HH, UK. E-mail: m.a.haniffa@ncl.ac.uk or x.n.wang@ncl.ac.uk

Abbreviations: APC, antigen-presenting cell; CTCL, cutaneous T-cell lymphoma; DC, dendritic cell; DEJ, dermoepidermal junction; GVHD, graft-versus-host disease; LC, Langerhans cell; Mϕ, macrophages

Received 16 June 2013; revised 25 September 2013; accepted 2 October 2013; accepted article preview online 11 November 2013; published online 19 December 2013

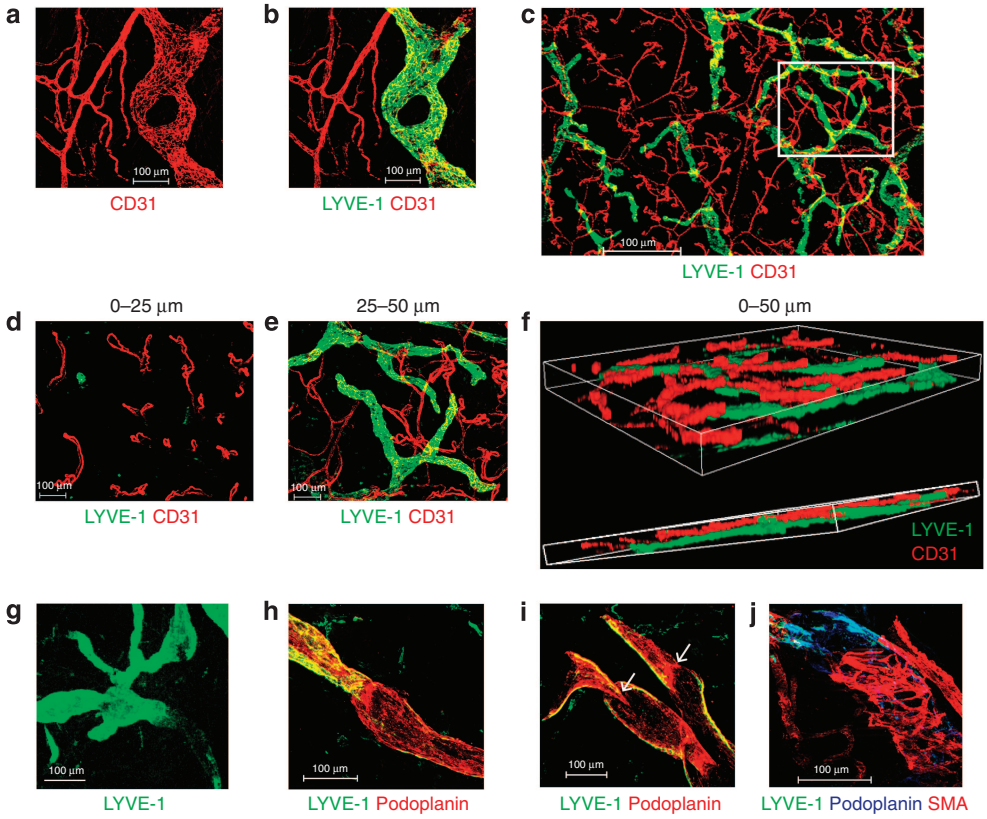

Figure 1. Dermal lymphatics and blood vessels. (**a**–**c**) CD31 (red) and LYVE-1 (green) staining to identify $CD31^+LYVE\text{-}1^-$ blood vessels and $CD31^{lo}LYVE\text{-}1^+$ lymphatic vessels. (**d**, **e**) Serial sections of region within inset in **c**. (**d**) $CD31^+$ capillary loops and $LYVE\text{-}1^+$ lymphatic tips at 0–25 μm. (**e**) Blood and lymphatic vessels between 25 and 50 μm beneath the dermoepidermal junction (DEJ). (**f**) A three-dimensional projection of **d** and **e**. (**g**) Loss of LYVE-1 (green) expression at the transition from initial to collecting lymphatic vessel (>500 μm beneath the DEJ). (**h**) $LYVE\text{-}1^+$ podoplanin$^+$ initial lymphatic vessels and $LYVE\text{-}1^{lo}$ podoplanin$^+$ collecting vessels. (**i**) Valves (white arrows) within collecting lymphatic vessels. (**j**) Smooth muscle actin (red) at the start of collecting lymphatic vessel. Data are representative of $n>5$ from >3 separate donors, maximum Z-stacks projection. Scale bar = 100 μm except **c** = 500 μm.

functional organization of interstitial leukocytes in normal and diseased skin.

RESULTS

Human dermis contains an interwoven network of lymphatic and blood vessels

We first assessed the distribution of dermal blood capillaries and lymphatics using antibodies to CD31 (PECAM1), an endothelial cell marker, and lymphatic vessel endothelial hyaluronan receptor 1 (LYVE-1). Double staining with CD31 and LYVE-1 allowed visualization of the blood capillary network ($CD31^+LYVE\text{-}1^-$) and initial lymphatics ($CD31^+LYVE\text{-}1^+$; Figure 1a–c). Looped blood capillaries were found in the first 25 μm beneath the dermoepidermal junction (DEJ; Figure 1d). Between 25 and 50 μm, blind-ended large bore lymphatics and capillary networks were easily visualized (Figure 1e). Whole-mount Z-stack reconstruction of the dermal whole mount to a depth of 50 μm beneath the DEJ showed the more superficial distribution of blood capillaries above the network of initial lymphatics (Figure 1f).

Initial lymphatic vessels appeared to lose LYVE-1 staining in deeper dermis (>500 μm) where intra-luminal valve-like structures were observed (Figure 1g). We analyzed the expression of the 38 kD transmembrane mucoprotein, podoplanin, reported to be expressed by both initial and collecting lymphatic vessels (Kawai and Ohhashi, 2012) and found that initial lymphatic vessels expressed both LYVE-1 and podoplanin, but collecting vessels were $LYVE\text{-}1^{lo/-}$ podoplanin$^+$ (Figure 1h). The transition between initial and collecting vessels was marked by intra-luminal valves (Figure 1i) and sparse expression of smooth muscle actin (Figure 1j).

Flow cytometry and cytology of dermal leukocytes

Before examining leukocytes *in situ*, we reviewed the phenotype, relative abundance, and morphology of dermal leukocytes by flow cytometry and cytology. Analysis of major histocompatibility complex class II expression (HLA-DR) and cell granularity (side scatter (SSC) parameter) enabled the separation of $HLA\text{-}DR^-SSC^{lo}CD3^+$ T lymphocytes from $HLA\text{-}DR^-SSC^{mid-hi}CD117^+$ mast cells and $HLA\text{-}DR^+$ APCs (Figure 2a). Mϕ were distinguishable by their autofluorescent properties from DCs (Figure 2a). Successive gating of the $HLA\text{-}DR^+$ autofluorescent-negative DC fraction allowed $CD14^+$ DCs to be separated from $CD14^-$ cells. The latter fraction comprises the major dermal $CD11c^{hi}$ DC population, which co-expressed CD1c (Haniffa *et al.*, 2009, 2012) and CD1a and $CD11c^{lo}CD141^{hi}$ DCs. $CD1a^{+++}$ LCs are $CD11c^{lo}CD141^{lo}$. $CD14^+$ DCs were shown to be functionally distinct from

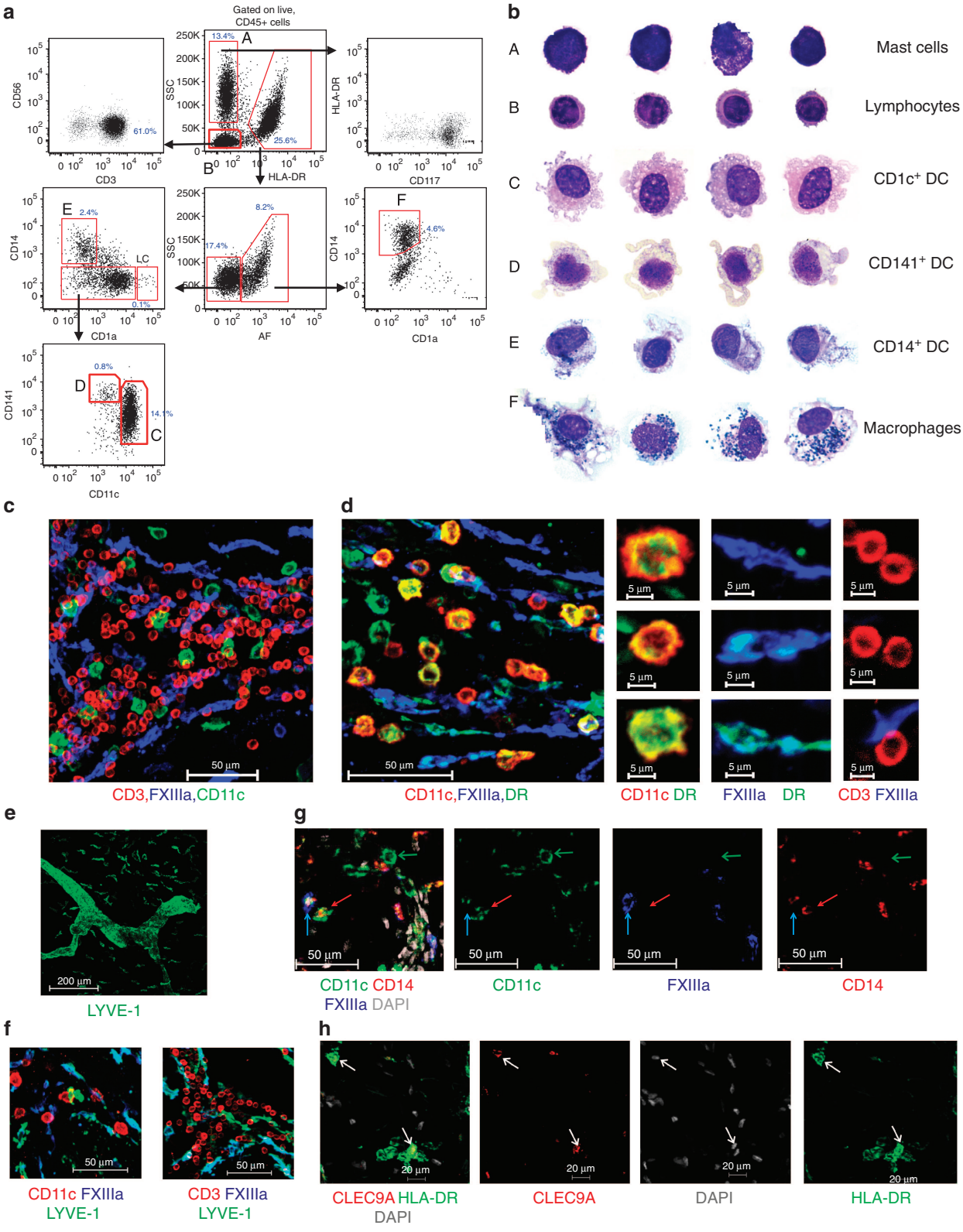

Figure 2. Flow cytometry, cytology, and *in situ* identification of dermal leukocytes. (**a**) Dermal leukocytes by flow cytometry as % of $CD45^+$ cells. Representative results from >3 experiments from >3 donors. (**b**) Cytology of dermal leukocytes. (**c**) CD11c (green; dendritic cell (DC)), CD3 (red; T cells), and FXIIIa (blue; Mϕ). (**d**) $CD11c^+$ DCs (red) are $HLA\text{-}DR^{br}$ (green), whereas $FXIIIa^+$ Mϕ (blue) are $HLA\text{-}DR^{lo/neg}$. Cropped images on right. (**e**) LYVE-1 (green) is expressed by Mϕ. (**f**) Some $FXIIIa^+$Mϕ express LYVE-1. (**g**) CD11c (green), CD14 (red), and FXIIIa (blue) distinguishes $CD11c^+CD14^-FXIIIa^{neg}$ DCs (green arrow) from $CD11c^+CD14^+FXIIIa^{lo-neg}$ DCs ($CD14^+$ DCs; red arrow) and $CD11c^-CD14^+$ $FXIIIa^{br}$ Mϕ (blue arrow). Scale bar = 50 µm. (**a–f**) Representative of $n>5$ from >3 separate donors. (**h**) $CLEC9A^+$(red) $HLA\text{-}DR^+$ (green) DCs (white arrows). Representative images from two donors. Maximum projection of Z-stacks shown.

dermal Mϕ by adherence, endocytosis, and migration out of skin explants cultured *ex vivo* (Haniffa *et al.*, 2009).

We confirmed the cellular identity of dermal leukocytes by Giemsa staining cytospin preparations of purified populations (Figure 2b). Mast cells and lymphocytes had a low cytoplasm to nuclear ratio. Mast cells had intensely basophilic cytoplasmic granules. Lymphocytes had circular nuclei with visible chromatin granules. Mϕ possessed highly vacuolated cytoplasm and dense blue–black cytoplasmic melanin granules, bean-shaped nucleus with lacy chromatin network. DCs had highly vacuolated acidophilic cytoplasm with characteristic fine external projections, an open nuclei with nucleoli consistent with replicative potential as previously reported (Haniffa *et al.*, 2009, 2012). In contrast, $CD14^+$ DCs had granular oval nuclei, a mildly vacuolated basophilic cytoplasm, and a few melanin granules in the occasional cell.

Dermal DCs, Mϕ, and T cells are phenotypically distinct *in situ*

We next sought to locate the dermal DC subsets, Mϕ, and T cells identified by flow cytometry and cytology *in situ*. Our previous analysis revealed the utility of the integrin, CD11c, and the transglutaminase FXIIIa, as antigens that distinguished DCs from Mϕ (Zaba *et al.*, 2007; Haniffa *et al.*, 2009). We used CD3 to identify T cells.

We detected a population of rounded $CD11c^+$ cells and a population of elongated cells that stained with FXIIIa (Figure 2c and d). There was no overlap between these two antigens with CD3. All $CD11c^+$ cells in the dermis were HLA-DR^+ and $CD3^-$ in keeping with the expected phenotype of DCs (Figure 2c and d). Mϕ were $CD11c^-$ and expressed variable HLA-DR (Figure 2d). DCs were larger compared with $CD3^+$ T cells and more rounded in shape and less elongated than dermal Mϕ, which were $FXIIIa^+$ HLA-DR^{lo} and $CD11c^-$ (Figure 2c and d). We also observed LYVE-1 expression on dermal Mϕ, although at a reduced level compared with lymphatic endothelium (Figure 2e). LYVE-1 colocalized, although incompletely, with $FXIIIa^+$ Mϕ and was not expressed by DCs or T cells (Figure 2f).

In addition, small numbers of perivascular cells expressing the lipopolysaccharide receptor CD14 and with a rounded morphology (Figure 2g) corresponding to migratory $CD14^+$ DCs known to express FXIIIa in common with dermal Mϕ (Nestle *et al.*, 1993; Klechevsky *et al.*, 2008; Haniffa *et al.*, 2009) were observed. These cells expressed higher CD14, but less FXIIIa than interstitial Mϕ (Figure 2g).

HLA-DR^+ $CLEC9A^+$ cells corresponding to $CD141^{hi}XCR1^+$ DCs as previously described (Haniffa *et al.*, 2012) were also identifiable *in situ* (Figure 2h). Both $CD14^+$ DCs and $CD141^{hi}XCR1^+$ DCs expressed CD11c (Figure 2g and Haniffa *et al.*, 2012). Migrating LCs were extremely rare and accounted for approximately 2% of $CD11c^+$ cells (Figure 2a and Supplementary Figure 1 online). As such, we used CD11c expression as a surrogate marker for all dermal DCs.

Anisotropic distribution of dermal DCs, Mϕ, and T cells

We next investigated the distribution of DCs, Mϕ, and T cells in the dermis. DCs were abundant at $<20\,\mu m$ beneath the DEJ (Figure 3a). Mϕ were more visible at 20–40 μm and persisted until 60 μm beneath the DEJ and formed a second cellular layer of APC (Figure 3b). T cells were found throughout the dermis but more abundant at 40–60 μm beneath the DEJ (Figure 3c). A three-dimensional reconstruction of the optical sections imaged up to 60 μm beneath the DEJ illustrates the cellular distribution of DCs, Mϕ, and T cells *in situ* (Figure 3d).

Below 60 μm, cells became progressively more organized in cords with an apparent perivascular distribution (see below). A convenient way to visualize deeper structures in the whole-mount dermal sheet was to examine the sheet from the subcutaneous face, which presented a level of about 150 μm (Figure 3e). DCs, Mϕ, and T cells located $>150\,\mu m$ beneath the DEJ were patchy in distribution with cell-dense and pauci-cellular areas (Figure 3e). The number of DCs, Mϕ, and T cells up to 30 μm beneath the DEJ per mm^2 dermis were 423 ± 168, 291 ± 51, and $1{,}153 \pm 231$, respectively (mean ± SD; Figure 3f). This equated to 7.62×10^8 DCs over an average total surface body area of $1.8\,m^2$, approximately 10-fold higher than the total number of myeloid DCs in the entire blood volume of 5 l ($7.5 \pm 3.02 \times 10^7$ myeloid DCs; Jardine *et al.* manuscript submitted). The number of T cells in the first 30 μm of dermis is estimated at $2.08 \pm 1.24 \times 10^9$ compared with $0.5–1 \times 10^{10}$ in 5 l of blood.

We next investigated the distribution of dermal CD8 and CD4 T lymphocytes. As CD4 is also expressed by DCs, double staining for CD3 and CD8 allowed us to identify $CD8^+$ T cells and $CD3^+CD8^-$ T cells (Figure 3g). In all, >90% of $CD3^+CD8^-$ T cells correspond to $CD4^+$ T helper cells as $CD3^+$ NKT cells are absent in healthy human skin (Figure 2a) and <10% of $CD3^+CD8^-$ dermal cells comprise γδT cells (Ebert *et al.*, 2006). We observed a higher proportion of $CD4^+$ T cells compared with $CD8^+$ T cells in the human dermis, in keeping with published data (Clark *et al.*, 2006a). The ratio of $CD8^+$: $CD4^+$ T cells was 1:2.9 at $<30\,\mu m$ and 1:4.1 at $>150\,\mu m$ beneath the DEJ.

DCs, Mϕ, and T cells have unique spatial relationships to dermal vessels

The organization of cells into cords suggested the existence of stable perivascular structures. Staining for CD31 with a cell marker revealed distinct spatial relationships of DCs, Mϕ, and T cells to the dermal vascular network (Figure 4a–d). In order to derive a quantitative view of the patterns of distribution, we compared apical ($<30\,\mu m$) with deep ($>150\,\mu m$) dermis. We enumerated DCs, Mϕ, and T cells that were perivascular ($<15\,\mu m$ from vessel) and interstitial ($>15\,\mu m$ from vessel). DCs found $<30\,\mu m$ beneath the DEJ were predominantly interstitial in distribution. However, at $>150\,\mu m$ beneath the DEJ, DCs were predominantly perivascular (Figure 4a). Mϕ were both perivascular and interstitial at $<30\,\mu m$ beneath the DEJ, but primarily perivascular at $>150\,\mu m$ beneath the DEJ (Figure 4b). T cells formed perivascular sheaths throughout the dermis (Figure 4c). DCs, Mϕ, and T cells did not have any specific spatial relationship with lymphatic vessels (Figure 4d). The ratio of DC:Mϕ:T cell at $<30\,\mu m$ beneath the DEJ was 1.0:0.5:2.2 but 1.0:1.2:5.02 at $>150\,\mu m$ beneath the DEJ. A schematic diagram to show the distribution of dermal leukocytes is illustrated in Figure 4e.

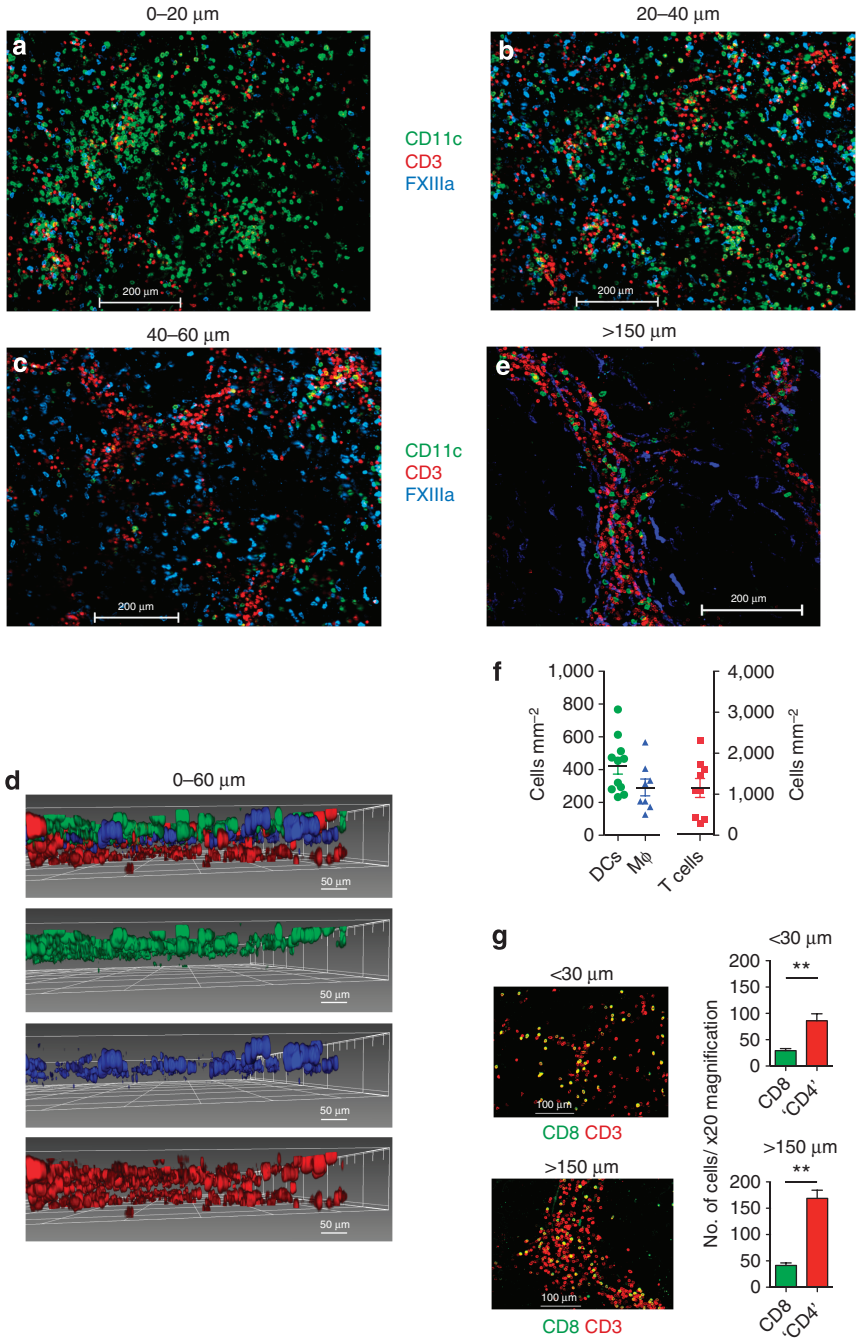

Figure 3. Anisotropic distribution of dermal leukocytes. Distribution of CD11c$^+$dendritic cells (DCs; green), FXIIIa$^+$ Mϕ (blue), and CD3$^+$ T cells (red) at (**a**) 0–20 μm, (**b**) 20–40 μm, and (**c**) 40–60 μm beneath the dermoepidermal junction (DEJ). (**d**) Three-dimensional reconstruction of **a–c**; DCs (green), Mϕ (blue), and T cells (red). (**e**) Distribution of CD11c$^+$ DCs, FXIIIa$^+$ Mϕ, and CD3$^+$ T cells at >150 μm beneath the DEJ. Scale bar = 200 μm except **d** = 50 μm. (**f**) Scatter plot of number of DCs, Mϕ, and T cells per mm^2 of dermis up to 30 μm depth. Each point is from one ×20 field; three fields per donor and 3–4 donors analyzed. (**g**) CD8$^+$ and CD3$^+$CD8$^-$ ("CD4$^+$") T cells at <30 μm and >150 μm beneath the DEJ. $P<0.001$. Mean ± SEM of six donors.

Apical dermal DCs with branching morphology express fascin

In healthy skin, some dermal DCs located more superficially (<20 μm beneath the DEJ) formed clusters of cells with highly branching cytoplasmic projections in contrast to DCs located >150 μm beneath the DEJ, which had a rounded morphology (Figure 5a and b). This led us to speculate whether the highly branching morphology was associated with increased activation and motility, a feature of lymphatic migration. We next interrogated dermal DCs for the expression of fascin, the actin cytoskeletal binding cell motility protein (Kureishy *et al.*, 2002). Interestingly, fascin was expressed exclusively by superficial DCs that were in clusters (Figure 5c). Fascin

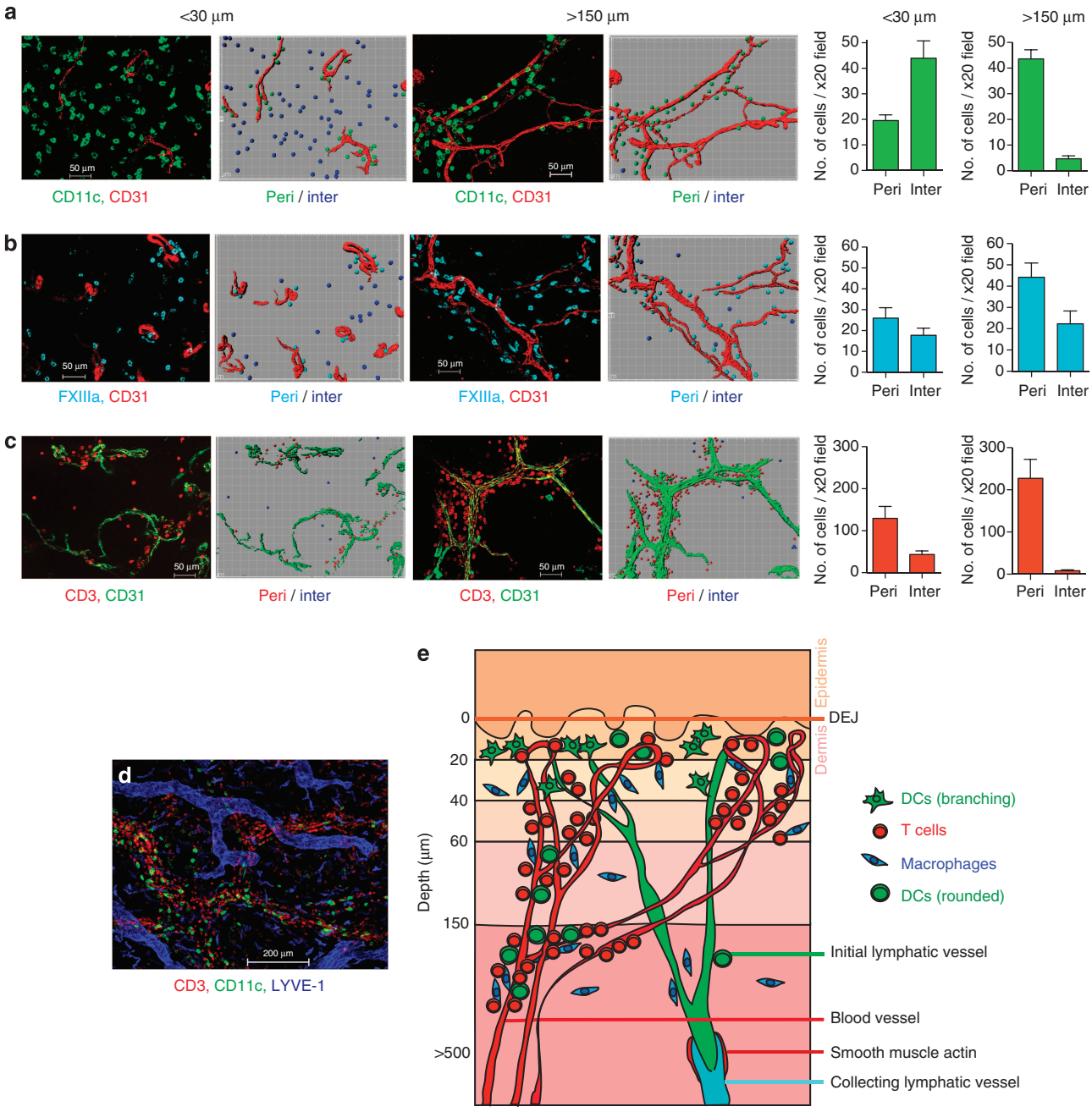

Figure 4. Relationship of dermal leukocytes to vascular structures. Distribution of (**a**) CD11c$^+$ dendritic cells (DCs; green), (**b**) FXIIIa$^+$ Mϕ (blue), and (**c**) CD3$^+$ T cells (red) in relation to blood vessels at <30 and >150 μm beneath the dermoepidermal junction (DEJ). Accompanying Imaris software representation is shown on the right. Bar graphs showing number of cells in ×20 field found in perivascular (peri; <15 μm from vessel) and interstitial (inter; >15 μm from vessel) distribution; mean ± SEM. (**d**) Distribution of CD11c$^+$ DC(green), LYVE-1$^+$ Mϕ (blue), and CD3$^+$ T cells (red) with lymphatic vessels (blue). Scale bar = 50 μm except **d** = 200 μm. Images are representative of >8 experiments, from >5 separate skin donors. (**e**) Schematic diagram illustrating the distribution of dermal leukocytes.

expression was found very rarely on DCs found perivascularly at >150 μm beneath the DEJ (Figure 5d). Mϕ did not express fascin (Figure 5e).

Dermal DCs but not Mϕ migrate into lymphatic vessels

We next performed dynamic studies of leukocyte migration into lymphatics. To our surprise, <1% of DCs were inside the lymphatic lumen in freshly isolated skin (Figure 5f). However, DCs were easily demonstrable within lymphatic lumen (>80% of DCs in field imaged) of dermal explants cultured for 32 hours *ex vivo* (Figure 5g). Consistent with our previous observations of fascin expression by highly branching DCs, we observed fascin upregulation on DCs migrating into lymphatics (Figure 5h). Mϕ did not express fascin and were never detected within dermal lymphatics in keeping with their resident fixed nature (Figure 5h).

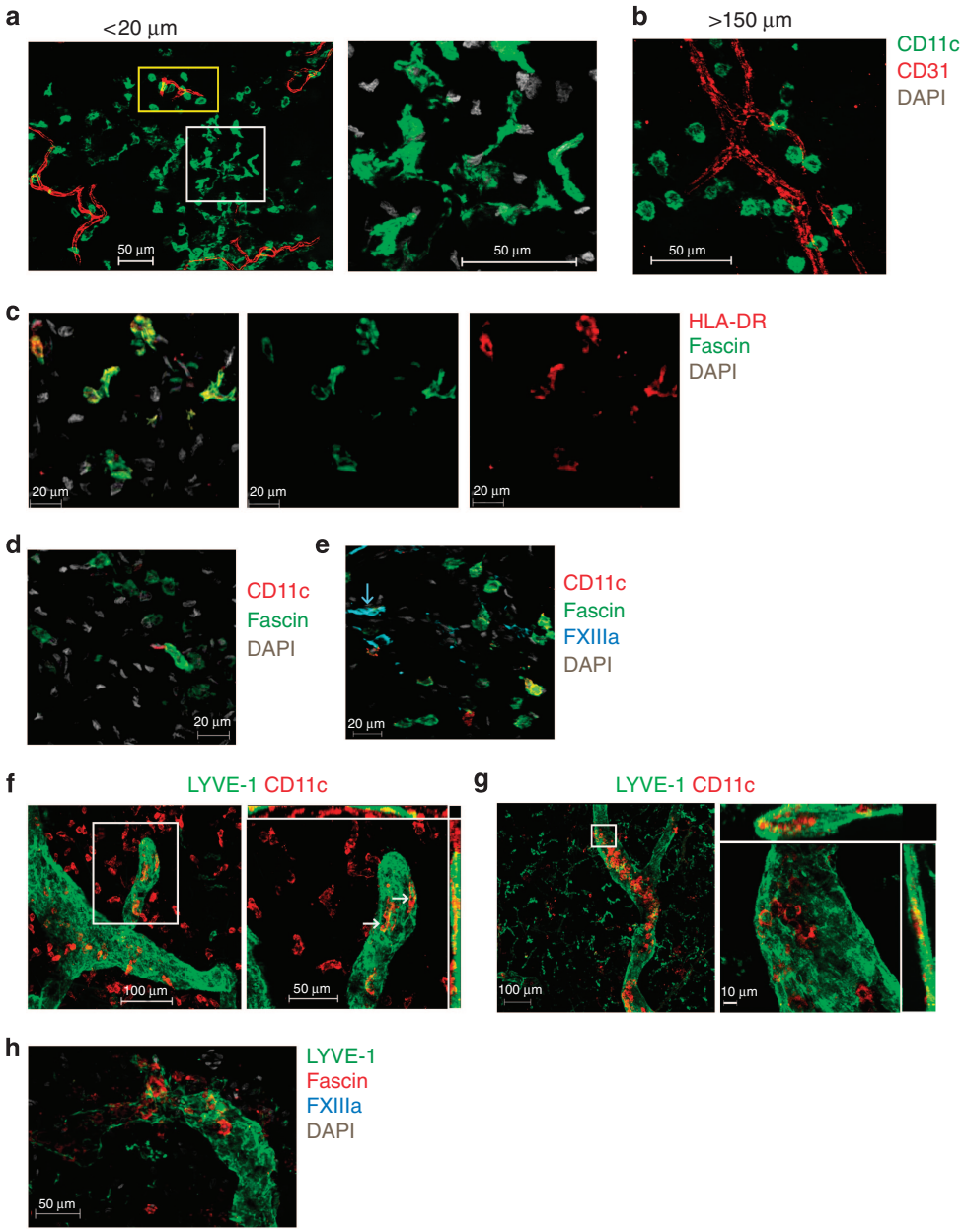

Figure 5. Dermal dendritic cells (DCs) migrate into lymphatics. (**a**) Apical CD11c$^+$ DCs (green) are rounded cells (yellow rectangle) with clusters of branching cells (white square; higher magnification in right panel). (**b**) CD11c$^+$ DCs (green) at >150 μm are round. (**c**) Branching apical CD11c$^+$ DCs (green) express fascin (red). (**d**) DCs (green) at >150 μm beneath the dermoepidermal junction (DEJ) very rarely express fascin (red). (**e**) FXIIIa$^+$ Mϕ (cyan) are fascin$^-$ (green). (**f**) <1% of CD11c$^+$ DCs (red) are inside LYVE-1$^+$ lymphatic vessels (green) in freshly isolated skin, but (**g**) >90% are detectable after 32 hours of skin explant culture. LYVE-1$^+$ Mϕ (green) are in the interstitium. White arrows indicate cells inside lymphatics in the orthogonal plane. Right panels are higher magnification of region within white rectangles. (**h**) Cells within LYVE-1$^+$ lymphatics (green) are FXIIIa$^-$ (cyan) and fascin$^+$ (red). Scale bar = 20 μm except **a, b** = 50 μm. Representative images from >3 experiments and donors.

Distortion of skin leukocyte architecture in disease

We next investigated dermal leukocyte microanatomy in disease. We imaged skin biopsies (<30 μm beneath the DEJ) from involved skin of patients with psoriasis, atopic dermatitis, CD4$^+$ cutaneous T-cell lymphoma (CTCL), and graft-versus-host disease (GVHD; Figure 6a–d). Psoriatic and atopic dermatitis skin exhibited cord-like leukocyte aggregates (Figure 6a and b) in contrast to the intense interstitial infiltrate seen in CTCL and GVHD (Figure 6c and d). There was a notable increase in DCs in addition to T cells in atopic dermatitis and GVHD (Figure 6b and d). DCs generally had a spindled or branched morphology in diseased skin. Although both CTCL and GVHD dermis were rich in DCs and T cells, a notable difference was the presence of lymphoid tissue-like aggregates in GVHD (Figure 6d) in contrast to the more diffuse infiltrate in CTCL (Figure 6c).

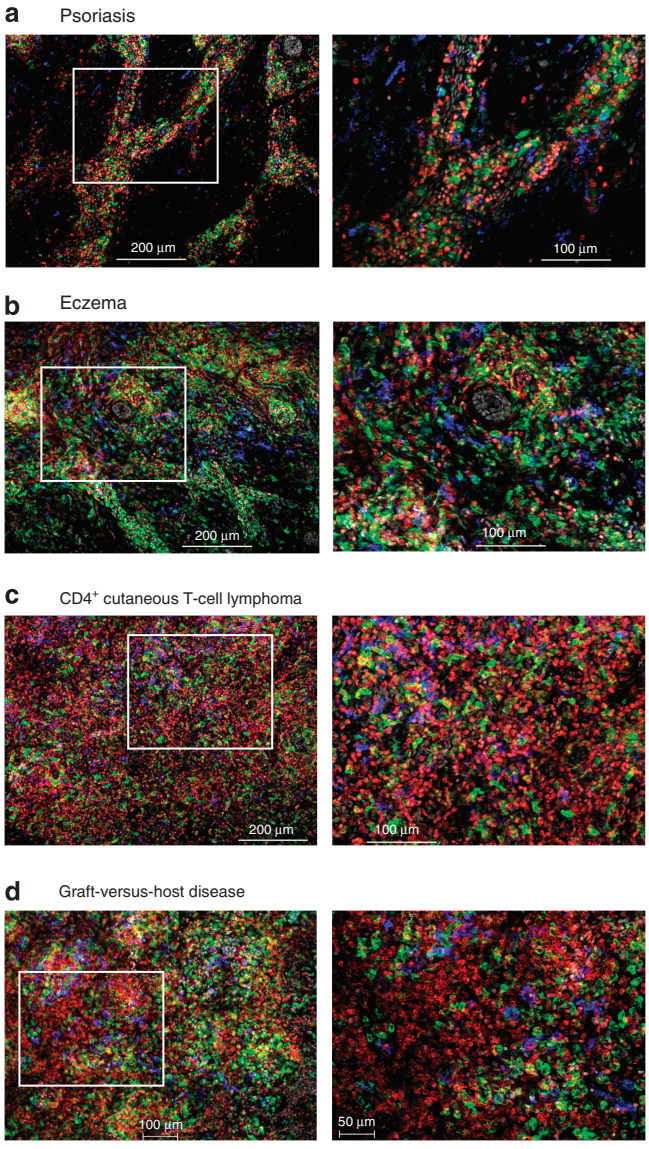

Figure 6. Dermal leukocyte architecture is distorted in disease. (**a**) Psoriasis, (**b**) atopic dermatitis, (**c**) cutaneous T cell lymphoma (CTCL), and (**d**) graft-versus-host disease (GVHD) skin showing $CD11c^+$ dendritic cells (DCs; green), $FXIIIa^+$ Mϕ (blue), and $CD3^+$ T cells (red); (scale bar = 200 μm except **d** = 100 μm left panel) and ×20 of white inset (scale bar = 100 μm except **d** = 50 μm right panel). Representative images from two to six independent donors.

DISCUSSION

This study provides a detailed analysis of the three-dimensional organization of leukocytes, blood, and lymphatic vessels within the human dermis. DCs, Mϕ, and T cells were differentially distributed by depth within the dermis and in relation to dermal vascular network. The whole-mount imaging analysis revealed the true extent of leukocytes in the dermis, previously underestimated using cross-section views. Stable perivascular sheaths of leukocytes can be observed in normal skin, but the leukocyte micro-anatomy is distorted in pathology and adopts disease-related patterns. In all, <1% of dermal DCs were located within dermal lymphatics in freshly isolated skin, but lymphatic migration were readily observed upon culturing skin *ex vivo*.

Lymphatic and blood vessel networks in the human dermis have been visualized by injecting vital dyes (Hudack and McMaster, 1933), electron microscopy (Sauter *et al.*, 1998), and more recently immunostaining for CD31, podoplanin, and LYVE-1 (Kriehuber *et al.*, 2001; Kawai and Ohhashi, 2012). The majority of these studies have focused on imaging skin by cross-section or *in vitro* cell culture analysis. Although intravital multiphoton imaging is useful for *in vivo* imaging of animal models (Tal *et al.*, 2011; Nagao *et al.*, 2012; Roediger *et al.*, 2013 and reviewed in Germain *et al.*, 2006), technical constraints have limited its application to study human tissue.

CD11c, FXIIIa, and CD3 identified DCs, Mϕ, and T cells in the dermis in agreement with previous reports (Zaba *et al.*, 2007; Ochoa *et al.*, 2008; Haniffa *et al.*, 2009). The spindle-shaped morphology of $FXIIIa^+$ Mϕ in the dermis had previously led to their initial characterization as ''dermal dendrocytes'' (Cerio *et al.*, 1989) and contrasts with $CD11c^+$ DCs, which are predominantly rounded *in situ*. Cytology provides additional distinction between DCs and Mϕ and confirms the characteristic cytoplasmic melanin granules seen in dermal Mϕ that visually describes the ''melanophage'' as shown here and in previous studies (McLellan *et al.*, 1998; Zaba *et al.*, 2007; Haniffa *et al.*, 2009). We also confirm that LYVE-1 is a receptor that can identify human dermal Mϕ as previously described (Bockle *et al.*, 2008; Attout *et al.*, 2009), although it does not colocalize completely with FXIIIa.

Our analysis of healthy human skin has been done using breast skin, and to avoid high autofluorescence of hair follicles we have focused on interfollicular areas. Our observation of distinct leukocyte layers and stable dermal perivascular sheaths of DCs, Mϕ, and T cells suggest the existence of microdomains where immune interactions occur. The recent demonstration in mice of long-lived skin resident effector memory T cells (Jiang *et al.*, 2012) and the role of skin-derived Tregs in inhibiting cutaneous immune response (Tomura *et al.*, 2010) highlights the potential significance of regional semi-autonomous immune regulation.

Although in cross-section dermal leukocytes appear enriched in the proximity of vascular structures (Cerio *et al.*, 1989; Zaba *et al.*, 2007; Ochoa *et al.*, 2008; Haniffa *et al.*, 2009), our data showing stable perivascular sheaths of leukocytes suggest positioning to interact with newly recruited leukocytes. DCs form the top most APC layer directly under the DEJ, which may relate to their role as surveyors of the DEJ.

As our quantification of DCs and T cells only takes into account the first 30 μm thickness of the dermis, the numbers we derive underestimate the true value. The abundance of T cells at >30 μm, anatomical sites sampled, and the lack of accounting for epidermal T cells may explain the discrepancy between our estimate and that previously reported (Clark *et al.*, 2006a, b). Nevertheless, the observation of high numbers of DCs in the skin compared with blood remains and is in keeping with their role as immune sentinels in peripheral tissues.

The expression of fascin by DCs has been reported to occur during DC maturation and migration to draining lymph node

(Ross *et al.*, 1998 and reviewed in Kureishy *et al.*, 2002). The association of clusters of fascin expressing DCs with extensive dendritic morphology at $<30\,\mu m$ beneath the DEJ suggests patrolling behavior or localized activation for lymphatic migration. Dynamic studies on tissue leukocytes in humans are technically challenging. Steady-state DC migration has been described as a mechanism to induce antigen tolerance (Steinman *et al.*, 2003) and reported using animal models (Laμmermann *et al.*, 2009; Tal *et al.*, 2011) and human lymphatic cannulation (Brand *et al.*, 1999). DCs in human skin explants cultured *in vitro* have been shown to form cords within the dermis and thought to reflect lymphatic migration (Lukas *et al.*, 1996). We detected very low numbers of DCs inside lymphatic vessels in freshly isolated skin, in agreement with observations in steady-state mouse skin (Ng *et al.*, 2008; Sen *et al.*, 2010), although a short intra-lymphatic transit time may obscure our detection capacity. Our analysis also confirms the lymphatic migratory property of dermal DCs in contrast to the tissue resident nature of Mϕ (Haniffa *et al.*, 2009). Previous studies on DC migration could not distinguish LCs from dermal DCs within lymphatics (Lukas *et al.*, 1996; Brand *et al.*, 1999). Further studies will be required to define the kinetics and understand the functional contribution of individual DC subsets in response to antigen challenge.

Our analysis of diseased skin focused on the superficial dermis. As human pDCs are $CD11c^-$, the infiltrating $CD11c^+$ cells we observed correspond to myeloid DCs. However, we cannot distinguish newly recruited ''inflammatory'' DCs from the ''steady-state'' DCs that are present in healthy skin. The surprising observation of DCs interspersed within $CD3^+$ T cells in CTCL skin suggests that lymphomatous T cells require growth stimulation or factors from adjacent cellular milieu. Epidermal changes in the different disorders will also accentuate the disease-related patterns we observed.

Our study demonstrates dermal leukocyte anisotropy in healthy human dermis, suggesting the existence of anatomical micro-domains that may have important functional and potentially exploitable properties. In addition, we show disease-related leukocyte topography, further advancing our understanding of the pathogenesis of inflammatory and malignant skin disorders.

MATERIALS AND METHODS

Preparation of whole mounts

Normal human skin was obtained with written informed consent from plastic surgery patients under approval of the Newcastle Research Ethics Committee and adherence to Helsinki Guidelines. Normal skin was obtained from patients undergoing mammoplasty aged between 18 and 65 years. Details for patients donating pathological skin are in Supplementary Table 1 online. Dermatome cut whole-skin sheets (200 μm thick) were fixed in 2% paraformaldehyde and 30% sucrose in phosphate-buffered saline overnight at 4 °C. Epidermis was separated by 1-hour incubation in $0.83\,mg\,ml^{-1}$ dispase (Gibco, Paisley, UK) at 37 °C. To image depths $>200\,\mu m$ beneath the DEJ, fixed skin sheet was optimal cutting temperature compound embedded and sectioned longitudinally (60–80 μm thickness). Dermal cell suspension for flow cytometry was prepared as previously described (Haniffa *et al.*, 2009).

Immunostaining and microscopy

Dermal sheets were blocked and permeabilized in phosphate-buffered saline containing 0.5% BSA, 0.3% TritionX-100 and washed with phosphate-buffered saline containing 0.2% BSA, 0.1% TritionX-100. Primary antibodies used were as follows: Ag (clone), supplied by BD Pharmingen (Oxford, UK) unless stated otherwise; CD3 (UCHT1); CD8 (HIT8a); CD11c (B-ly6); CD11c-FITC (BU15; AbDSerotec, Kidlington, UK); CD14 (polyclonal; Sigma, Dorset, UK); CD31 (WM59); FXIIIa (polyclonal; Enzyme Research, Swansea, UK); LYVE-1 (polyclonal; R&D, Minneapolis, MN); α-smooth muscle actin (1A4; Sigma); podoplanin (polyclonal; R&D); HLA-DR (G46-6); HLA-DR-FITC (L243); CLEC9A (8F9; Miltenyi Biotec, Bisley, UK); fascin (55K2; Abcam, Cambridge, UK). Secondary antibodies used were as follows: donkey anti-sheep, donkey anti-mouse, and donkey anti-goat Dy488, Dy549, and Dy649 (Jackson ImmunoResearch, Suffolk, UK), AlexaFluor555 or AlexaFluor647 (Invitrogen, Paisley, UK), and Streptavidin-Cy2 or Cy5 (Jackson ImmunoResearch). Biotinylation of primary antibody was performed using TSA Biotin staining kit (Perkin Elmer, Cambridge, UK). Tissue sections were immersed in Vecta mounting medium with 4,6-diamidino-2-phenylindole (Vector Laboratories, Peterborough, UK) for 3 hours before analysis.

Ex vivo DC migration assay

Skin sheets was placed in RPMI with 10% fetal calf serum at 37 °C for 32 hours before paraformaldehyde fixation and staining as described above.

Microscopy and cell count

The immunostained specimens were imaged using AxioImager.Z2 fluorescence microscope with Axiovision software v4.8 (Carl Zeiss, Jena, Germany). Epidermis side up was imaged and the tissue turned to scan dermal face. Three-dimensional reconstruction of the dermis and leukocyte enumeration were performed using Imaris7.6.2 software (www.bitplane.com).

Flow cytometry

Antibodies were obtained from BD (Oxford, UK) unless stated otherwise. Antigen (clone): CD1aAPC (HI149); CD3PE (SK7); CD11cA700 (B-Ly6); CD14PE and PECy7 (M5E2); CD45APC (H130); CD45APCCy7 (2D1); CD117PE (104D2); CD141PE and APC (Miltenyi, Bisley, UK; AD5-14H12); and HLA-DRPerCPCy5.5 (L243). Flow cytometry was performed using BD LSRII and the data analyzed with FlowJo (Treestar, Ashland, OR). Cytospin preparation and Giemsa staining were performed as previously described (Haniffa *et al.*, 2009)

Statistical analysis

Statistical analysis was carried out using two-tailed nonparametric Mann–Whitney *U*-test (PrismV5, La Jolla, CA). $P<0.05$ was considered significant.

CONFLICT OF INTEREST

The authors state no conflict of interest.

ACKNOWLEDGMENTS

This study was funded by the Wellcome Trust (WT088555) and Tyneside Leukaemia Research Association. We thank Dr Trevor Booth and Dr Alex Laude for bio-imaging, Dr Xin Xu for tissue processing, and the support of

Professor Peter Farr, Dr Sophie Weatherhead, Dr John Frew, Dr Clifford Lawrence, and Dr Khadija Al-Jefri from the Department of Dermatology and Oncology, Newcastle upon Tyne NHS Trust.

SUPPLEMENTARY MATERIAL

Supplementary material is linked to the online version of the paper at http://www.nature.com/jid

REFERENCES

Attout T, Hoerauf A, Denece G *et al.* (2009) Lymphatic vascularisation and involvement of Lyve-1 + macrophages in the human onchocerca nodule. *PLoS One* 4:e8234

Bockle BC, Solder E, Kind S *et al.* (2008) DC-sign + CD163 + macrophages expressing hyaluronan receptor LYVE-1 are located within chorion villi of the placenta. *Placenta* 29:187–92

Brand CU, Hunger RE, Yawalkar N *et al.* (1999) Characterization of human skin-derived CD1a-positive lymph cells. *Arch Dermatol Res* 291:65–72

Cerio R, Griffiths CE, Cooper KD *et al.* (1989) Characterization of factor XIIIa positive dermal dendritic cells in normal and inflamed skin. *Br J Dermatol* 121:421–31

Clark RA (2010) Skin-resident T cells: the ups and downs of on site immunity. *J Invest Dermatol* 130:362–70

Clark RA, Chong B, Mirchandani N *et al.* (2006a) The vast majority of CLA + T cells are resident in normal skin. *J Immunol* 176:4431–9

Clark RA, Chong BF, Mirchandani N *et al.* (2006b) A novel method for the isolation of skin resident T cells from normal and diseased human skin. *J Invest Dermatol* 126:1059–70

Collin M, McGovern N, Haniffa M (2013) Human dendritic cell subsets. *Immunology* 140:22–30

Czernielewski JM, Schmitt D, Faure MR *et al.* (1983) Functional and phenotypic analysis of isolated human Langerhans cells and indeterminate cells. *Br J Dermatol* 108:129–38

Eyerich S, Eyerich K, Pennino D *et al.* (2009) Th22 cells represent a distinct human T cell subset involved in epidermal immunity and remodeling. *J Clin Invest* 119:3573–85

Ebert LE, Meuter S, Moser B (2006) Homing and function of human skin gd T cells and NK cells: relevance for tumour surveillance. *J Immunol* 176:4431–6

Forster R, Braun A, Worbs T (2012) Lymph node homing of T cells and dendritic cells via afferent lymphatics. *Trends Immunol* 33:271–80

Germain RN, Miller MJ, Dustin ML *et al.* (2006) Dynamic imaging of the immune system: progress, pitfalls and promise. *Nat Rev Immunol* 6:497–507

Haniffa M, Ginhoux F, Wang XN *et al.* (2009) Differential rates of replacement of human dermal dendritic cells and macrophages during hematopoietic stem cell transplantation. *J Exp Med* 206:371–85

Haniffa M, Shin A, Bigley V *et al.* (2012) Human tissues contain CD141(hi) cross-presenting dendritic cells with functional homology to mouse CD103(+) nonlymphoid dendritic cells. *Immunity* 37:60–73

Hudack SS, McMaster PD (1933) The lymphatic participation in human cutaneous phenomena: a study of the minute lymphatics of the living skin. *J Exp Med* 57:751–74

Jiang X, Clark RA, Liu L *et al.* (2012) Skin infection generates non-migratory memory CD8 + T(RM) cells providing global skin immunity. *Nature* 483: 227–31

Kawai Y, Ohhashi T (2012) Current topics of immunohistochemical and biological properties of human lymphatic endothelial cells. *Ann Vasc Dis* 5:269–74

Klechevsky E, Morita R, Liu M *et al.* (2008) Functional specializations of human epidermal langerhans cells and CD14 + dermal dendritic cells. *Immunity* 29:497–510

Kriehuber E, Breiteneder-Geleff S, Groeger M *et al.* (2001) Isolation and characterization of dermal lymphatic and blood endothelial cells reveal stable and functionally specialized cell lineages. *J Exp Med* 194:797–808

Kureishy N, Sapountzi V, Prag S *et al.* (2002) Fascins, and their roles in cell structure and function. *Bioessays* 24:350–61

Laµmermann T, Renkawitz J, Wu X *et al.* (2009) Cdc42-dependent leading edge coordination is essential for interstitial dendritic cell migration. *Blood* 113:5703–10

Lenz A, Heine M, Schuler G *et al.* (1993) Human and murine dermis contain dendritic cells. Isolation by means of a novel method and phenotypical and functional characterization. *J Clin Invest* 92:2587–96

Lukas M, Stossel H, Hefel L *et al.* (1996) Human cutaneous dendritic cells migrate through dermal lymphatic vessels in a skin organ culture model. *J Invest Dermatol* 106:1293–9

McLellan AD, Heiser A, Sorg RV *et al.* (1998) Dermal dendritic cells associated with T lymphocytes in normal human skin display an activated phenotype. *J Invest Dermatol* 111:841–9

Morelli AE, Rubin JP, Erdos G *et al.* (2005) CD4 + T cell responses elicited by different subsets of human skin migratory dendritic cells. *J Immunol* 175:7905–15

Nagao K, Kobayashi T, Moro K *et al.* (2012) Stress-induced production of chemokines by hair follicles regulates the trafficking of dendritic cells in skin. *Nat Immunol* 13:744–52

Nestle FO, Zheng XG, Thompson CB *et al.* (1993) Characterization of dermal dendritic cells obtained from normal human skin reveals phenotypic and functionally distinctive subsets. *J Immunol* 151: 6535–45

Ng LG, Hsu A, Mandell MA *et al.* (2008) Migratory dermal dendritic cells act as rapid sensors of protozoan parasites. *PLoS Pathog* 4:e1000222

Ochoa MT, Loncaric A, Krutzik SR *et al.* (2008) "Dermal dendritic cells" comprise two distinct populations: CD1(+) dendritic cells and CD209(+) macrophages. *J Invest Dermatol* 128:2225–31

Roediger B, Kyle R, Yip KH *et al.* (2013) Cutaneous immunosurveillance and regulation of inflammation by group 2 innate lymphoid cells. *Nat Immunol* 14:564–73

Ross R, Ross XL, Schwing J *et al.* (1998) The actin-bundling protein fascin is involved in the formation of dendritic processes in maturing epidermal Langerhans cells. *J Immunol* 160:3776–82

Sallusto F, Zielinski CE, Lanzavecchia A (2012) Human Th17 subsets. *Eur J Immunol* 42:2215–20

Sauter B, Foedinger D, Sterniczky B *et al.* (1998) Immunoelectron microscopic characterization of human dermal lymphatic microvascular endothelial cells. Differential expression of CD31, CD34, and type IV collagen with lymphatic endothelial cells vs blood capillary endothelial cells in normal human skin, lymphangioma, and hemangioma in situ. *J Histochem Cytochem* 46:165–76

Sen D, Forrest L, Kepler TB *et al.* (2010) Selective and site-specific mobilization of dermal dendritic cells and Langerhans cells by Th1- and Th2-polarizing adjuvants. *Proc Natl Acad Sci USA* 107:8334–9

Seneschal J, Clark RA, Gehad A *et al.* (2012) Human epidermal Langerhans cells maintain immune homeostasis in skin by activating skin resident regulatory T Cells. *Immunity* 36:873–84

Steinman RM, Hawiger D, Nussenzweig MC *et al.* (2003) Tolerogenic dendritic cells. *Annu Rev Immunol* 21:685–711

Tal O, Lim HY, Gurevich I *et al.* (2011) DC mobilization from the skin requires docking to iµmobilized CCL21 on lymphatic endothelium and intralymphatic crawling. *J Exp Med* 208:2141–53

Tomura M, Honda T, Tanizaki H *et al.* (2010) Activated regulatory T cells are the major T cell type emigrating from the skin during a cutaneous immune response in mice. *J Clin Invest* 120:883–93

Zaba LC, Fuentes-Duculan J, Steinman RM *et al.* (2007) Normal human dermis contains distinct populations of CD11c + BDCA-1 + dendritic cells and CD163 + FXIIIA + macrophages. *J Clin Invest* 117:2517–25

Zaba LC, Krueger JG, Lowes MA (2009) Resident and "inflammatory" dendritic cells in human skin. *J Invest Dermatol* 129:302–8